Dovepress
Taylor & Francis Group

ORIGINAL RESEARCH

Development and Validation of a Diagnostic Model for Stanford Type B Aortic Dissection Based on Proteomic Profiling

Zihe Zhao[1,]*, Taicai Chen[2,3,]*, Qingyuan Liu[4], Jianhang Hu[1], Tong Ling[2,3], Yuanhao Tong[5], Yuexue Han[1], Zhengyang Zhu[6], Jianfeng Duan[7], Yi Jin[1], Dongsheng Fu[1], Yuzhu Wang[1], Chaohui Pan[1], Reyaguli Keyoumu[1], Lili Sun[1], Wendong Li[1], Xia Gao[8,9], Yinghuan Shi[2,3], Huan Dou [10,11], Zhao Liu[1]

[1]Department of Vascular Surgery, Nanjing Drum Tower Hospital, Affiliated Hospital of Medical School, Nanjing University, Nanjing, People's Republic of China; [2]The State Key Laboratory for Novel Software Technology, Nanjing University, Nanjing, People's Republic of China; [3]National Institute of Healthcare Data Science, Nanjing University, Nanjing, People's Republic of China; [4]Department of Neurosurgery, Beijing Tiantan Hospital, Capital Medical University, Beijing, People's Republic of China; [5]Department of Thoracic Surgery, BenQ Medical Center, Affiliated BenQ Hospital of Nanjing Medical University, Nanjing, Jiangsu, People's Republic of China; [6]Department of Radiology, Nanjing Drum Tower Hospital, Affiliated Hospital of Medical School, Nanjing University, Nanjing, People's Republic of China; [7]Department of Critical Care Medicine, Nanjing Drum Tower Hospital, Affiliated Hospital of Medical School, Nanjing University, Nanjing, People's Republic of China; [8]Department of Otolaryngology, Head and Neck Surgery, Nanjing Drum Tower Hospital, Affiliated Hospital of Medical School, Nanjing University, Nanjing, People's Republic of China; [9]Jiangsu Provincial Key Medical Discipline (Laboratory), Nanjing Drum Tower Hospital, Affiliated Hospital of Medical School, Nanjing University, Nanjing, People's Republic of China; [10]The State Key Laboratory of Pharmaceutical Biotechnology, Division of Immunology, Medical School, Nanjing University, Nanjing, People's Republic of China; [11]Jiangsu Key Laboratory of Molecular Medicine, Medical School, Nanjing University, Nanjing, People's Republic of China

*These authors contributed equally to this work

Correspondence: Zhao Liu, Department of Vascular Surgery, Nanjing Drum Tower Hospital, Affiliated Hospital of Medical School, Nanjing University, #321 Zhongshan Road, Nanjing, 210008, People's Republic of China, Email liuzhao@nju.edu.cn; Huan Dou, The State Key Laboratory of Pharmaceutical Biotechnology, Division of Immunology, Medical School, Nanjing University, Nanjing, People's Republic of China, Email douhuan@nju.edu.cn

Purpose: Stanford Type B Aortic Dissection (TBAD), a critical aortic disease, has exhibited stable mortality rates over the past decade. However, diagnostic approaches for TBAD during routine health check-ups are currently lacking. This study focused on developing a model to improve the diagnosis in a population.

Patients and Methods: Serum biomarkers were investigated in 88 participants using proteomic profiling combined with machine learning. The findings were validated using ELISA in other 80 participants. Subsequently, a diagnostic model for TBAD integrating biomarkers with clinical indicators was developed and assessed using machine learning.

Results: Six differentially expressed proteins (DEPs) were identified through proteomic profiling and machine learning in discovery and derivation cohorts. Five of these (GDF-15, IL6, CD58, LY9, and Siglec-7) were further verified through ELISA validation within the validation cohort. In addition, ten blood-related indicators were selected as clinical indicators. Combining biomarkers and clinical indicators, the machine learning-based models performed well (AUC of the biomarker model = 0.865, AUC of the clinical model = 0.904, and AUC of the combined model = 0.909) using relative quantitation. The performance of the three models was verified (AUC of biomarker model = 0.866, AUC of clinical model = 0.868, and AUC of combined model = 0.886) using absolute quantitation. Crucially, the combined models outperformed individual biomarkers and clinical models, demonstrating superior efficacy.

Conclusion: Using proteomic profiling, we identified serum IL-6, GDF-15, CD58, LY9, and Siglec-7 as TBAD biomarkers. The machine-learning-based diagnostic model exhibited significant potential for TBAD diagnosis using only blood samples within the population.

Keywords: type B aortic dissection, proteomics, machine learning, serum biomarkers, diagnostic model

533

Introduction

Stanford type B aortic dissection (TBAD) is a common, life-threatening condition originating distal to the left subclavian artery, accounting for 25%–40% of all aortic dissections.[1,2] Characterized by rapid onset, progression, and a high risk of rupture, TBAD often leads to organ failure.[3] The global incidence is 1.6 per 100,000 persons/year.[4] Despite advances in diagnosis and management, TBAD mortality remains stable, in contrast to the decline in type A aortic dissection (TAAD).[5] Aorta-related adverse events during the chronic phase of TBAD worsen the long-term outcomes and create a significant societal burdens.[6] Therefore, early and effective diagnosis within a population is crucial.

TBAD diagnosis primarily relies on imaging techniques such as transesophageal echocardiography (TEE), CT angiography (CTA), and magnetic resonance imaging (MRI).[7–9] However, these methods are not suitable for diagnosis of TBAD during routine health checkups due to their high cost, invasiveness, and radiation exposure risks.[10,11] Changes in plasma protein expression offer a noninvasive, cost-effective alternative that reflects human physiology and pathology.[12–14] Although several serum biomarkers for aortic dissection have been identified (soluble ST2, etc.),[15–17] their diagnostic efficiency in TBAD remains unproven.[18,19] Moreover, multi-biomarker integration is considered as a promising diagnostic enhancement for cardiovascular diseases recently.[18]

Traditional techniques, such as electrophoresis, ELISA, and mass spectrometry, have limitations including complex experimental stages and low sample throughput.[20] Less than 15 proteins accounted for over 90% of the serum protein content.[21] High-throughput antibody microarray excels in detecting low-abundance proteins,[22] making it ideal for serum biomarker screening.[23,24] Machine learning offers a robust approach to proteomic data analysis, enabling the development of reliable diagnostic models.[25–27] Multiple previous studies have applied machine learning to identify specific biomarkers of several diseases and achieved ideal effect, such as alcohol-related liver disease,[28] Parkinson's disease,[29] coronary artery disease[30] and progressive fibrosing interstitial lung disease.[31] Integrating proteomic profiling using antibody microarrays with machine learning offers a promising strategy for disease diagnosis,[32] facilitating to the identification of biomarkers for TBAD.

In this study, we attempted to develop a diagnostic model for TBAD based on serum biomarkers and clinical indicators that could be applied to routine health checkups and improve the early detection of TBAD. We investigated potential biomarkers among 1000 serum proteins using high-throughput proteomics and machine learning and verified our findings with ELISA in an independent cohort. We then used machine learning methods to develop a TBAD diagnostic model integrating these biomarkers with clinical indicators, and validated its performance in an independent cohort.

Material and Methods

Study Design

The study design, depicted in Figure 1, aimed to identify TBAD biomarkers and to develop a diagnostic model. Three Chinese cohorts diagnosed with TBAD were enrolled for biomarker discovery and validation. Initially, 1000 serum proteins (including interleukins, chemokines, tumor necrosis factor superfamily, growth factors, and colony-stimulating factors) were evaluated using commercial antibody arrays from RayBiotech. Differentially expressed proteins (DEPs) were identified in an 8-participant cohort and were later confirmed in an 80-participant cohort. A high-performance machine learning algorithm was employed to enhance biomarker identification and predictive accuracy. Subsequently, the selected biomarkers were validated by ELISA in an independent cohort. Stable biomarkers that demonstrated significant differences between the patients and controls were confirmed to be TBAD-specific. The final phase involved establishing a comprehensive diagnostic model for TBAD by integrating both biomarkers and clinical indicators.

Study Population

A summary of the clinical cohort is shown in Figure 1. We aimed to identify potential serum biomarkers on a large scale by collecting samples and clinical data from a discovery cohort of eight individuals (five patients with TBAD and three healthy controls) between May and July 2022. The derivation cohort included 80 participants (50 patients with TBAD and 30 healthy controls) from September 2022 to February 2023. The baseline patient characteristics are presented in
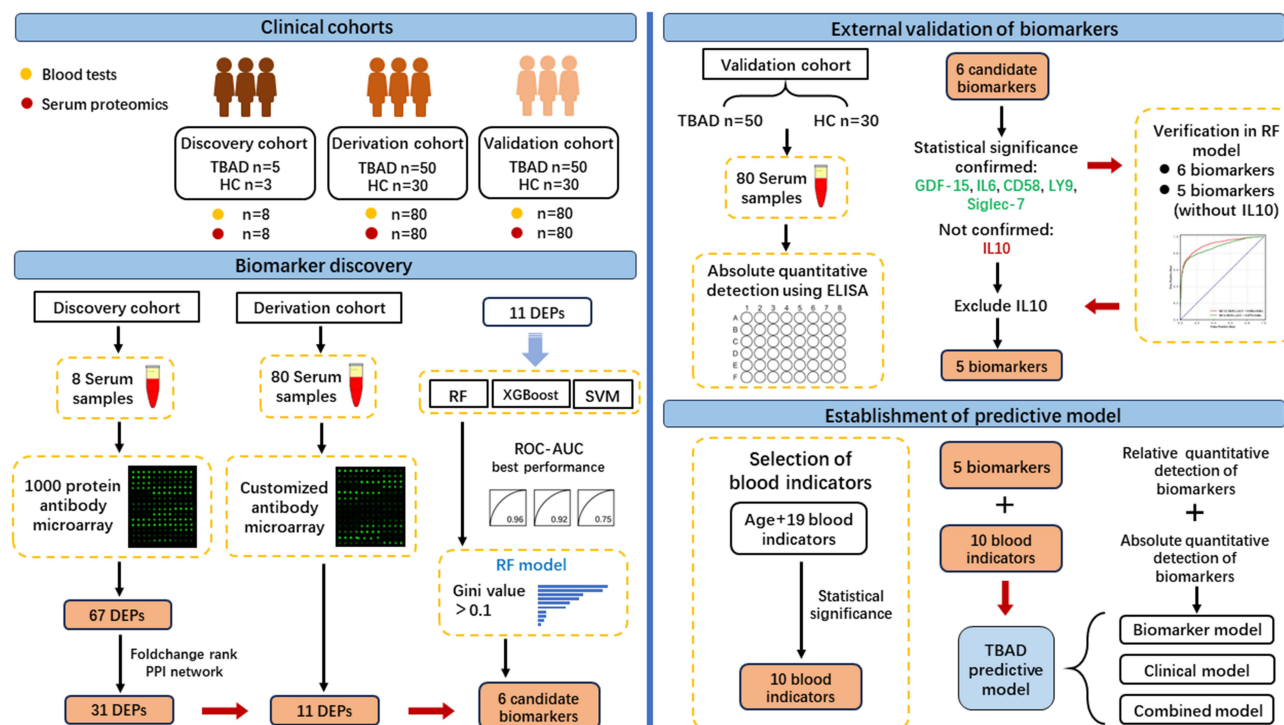
Figure 1 Study design.
Abbreviations: TBAD, type B aortic dissection; HC, healthy control; DEPs, differentially expressed proteins; PPI network, protein-protein interaction network; RF, random forest; XGBoost, eXtreme Gradient Boost; SVM, support vector machine.

Table 1. An independent validation cohort comprised of 50 patients with TBAD and 30 healthy controls recruited between April and November 2023 (Table 2).

TBAD diagnosis followed the criteria of the European Society of Cardiology (ESC) and standards of the Society for Vascular Surgery (SVS) and Society of Thoracic Surgeons (STS).[3,7] The inclusion criteria for patients with TBAD were age > 18 years, onset within two weeks, and radiological diagnosis. The exclusion criteria were severe infectious

Table 1 Baseline Characteristics of Participants in Discovery and Derivation Cohorts

Characteristics	Patients with TBAD (n=55)	Healthy Control (n=33)	P Value
Age (mean [SD])	53.9 (9.0)	50.1 (9.8)	0.0665
Sex (%)			0.6464
Male	51 (92.7)	32 (96.9)	
Female	4 (7.3)	1 (3.1)	
Hypertension (%)	45 (81.8)	23 (69.7)	0.2013
Diabetes (%)	2 (3.6)	2 (6.1)	0.6287
Hyperlipidemia (%)	5 (9.1)	2 (6.1)	0.7069
Atherosclerosis (%)	2 (3.6)	1 (3.0)	>0.9999
History of stroke (%)	3 (5.5)	0 (0)	0.2888
CAD (%)	2 (3.6)	0 (0)	>0.9999
COPD (%)	1 (1.8)	0 (0)	>0.9999
Renal insufficiency (%)	2 (3.6)	1 (3.0)	>0.9999
Smoking (%)	16 (29.1)	11 (33.3)	0.8118

Notes: Data are presented as mean [SD] for continuous variables and number (%) for categorical variables.
Abbreviations: CAD, coronary artery disease; COPD, chronic obstructive pulmonary disease.

Table 2 Baseline Characteristics of Participants in Validation Cohort

Characteristics	Patients with TBAD (n=50)	Healthy Control (n=30)	P Value
Age (mean [SD])	53.5 (12.1)	49.5 (10.2)	0.1395
Sex (%)			>0.9999
Male	45 (90.0)	27 (90.0)	
Female	5 (10.0)	3 (10.0)	
Hypertension (%)	41 (82.0)	24 (80.0)	>0.9999
Diabetes (%)	5 (10.0)	2 (6.7)	0.7057
Hyperlipidemia (%)	3 (6.0)	1 (4.8)	>0.9999
Atherosclerosis (%)	1 (2.0)	0 (0)	>0.9999
History of stroke (%)	6 (6.0)	0 (0)	0.0786
CAD (%)	0 (0)	0 (0)	>0.9999
COPD (%)	0 (0)	0 (0)	>0.9999
Renal insufficiency (%)	6 (8.0)	1 (3.3)	0.2464
Smoking (%)	16 (32.0)	9 (30.0)	>0.9999

Notes: Data are presented as mean [SD] for continuous variables and number (%) for categorical variables.
Abbreviations: CAD, coronary artery disease; COPD, chronic obstructive pulmonary disease.

diseases, other aortic diseases, Marfan syndrome, rheumatoid autoimmune diseases, cancer, mental illnesses, prior surgical interventions, or medical therapy. Healthy controls met the following criteria: no aortic diseases, age eighteen or older, no prior surgeries, and absence of cardiovascular or cerebrovascular diseases, with exclusion based on current infectious diseases, rheumatoid autoimmune diseases, cancer, mental illnesses, pregnancy or lactation, or no prior use of anti–infection or anti-inflammatory medications before admission.

Serum Sample and Clinical Indicators Collection
The participants fasted for eight hours prior to blood collection. Blood samples were collected within 12 h of admission and divided into tubes for common tests and proteomic profiling. The serum was centrifuged at 2500 rpm for ten minutes at 4°C within 12 h and stored at −80°C to prevent thaw-refreeze cycles. Post-centrifugation haemolyzed samples were excluded to avoid any detection bias. Blood tests, including sex, age, and comprehensive parameters such as cell counts, hemoglobin concentrations, and lipid levels, were completed within two days (Table S1). All data were documented for further analysis.

Antibody Microarray Assay
To screen DEPs among 1000 serum proteins, we used RayBio® G-Series Antibody Microarrays for relative quantification. Serum samples from patients with TBAD (n = 5) and healthy controls (n = 3) were used for the initial discovery study. Then, we employed RayBio® Custom Human Antibody Arrays for the derivation study and identified potential serum biomarkers, using samples from patients with TBAD (n = 50) and healthy controls (n = 30). These experiments were conducted following the manufacturer's protocol. The array slides were treated with 100 μL of 1X Blocking Buffer and incubated at room temperature (RT) for 30 min. We then added 50–100 μL of each two-fold diluted sample to each sub-array for a two-hour incubation at RT, followed by sequential washing with wash buffers I and II. Biotin-conjugated anti-cytokine and streptavidin-Fluor were applied for two hours each at RT. The slides were scanned in the cy3 or "green" channel using an InnoScan 300 Microarray Scanner. Raw data, including spot intensities, were exported and analyzed using RayBio Analysis Tool software for comprehensive protein expression evaluation.

Proteomic Profiling and Function Analysis
Data processing was performed using the open-source R and RStudio software. We utilized ggplot2 and ggfortify for scatter and volcano plots and principal component analysis (PCA) with prcomp and autoplot to identify data patterns.

Cluster heatmaps were generated using heatmap.2 in the gplots package. DEPs screening employed the limma package to evaluate the adjusted p-values and log2 fold changes (logFC).

Raw data were subjected to log2 transformation for normalization. DEPs were identified using a moderated t-statistic and adjusted using the Benjamini-Hochberg method to control false discovery rates (P < 0.05, fold change > 1.2, and average fluorescence signal value per group > 150). Gene Ontology (GO) and KEGG pathways were analyzed using Fisher's exact test with clusterProfiler. The DEPs for the Protein-Protein Interaction (PPI) were mapped to the STRING database (version 12.0). Finally, hub gene analysis was performed using the Maximal Clique Centrality (MCC) ranking from Cytoscape software (version 3.9.1).

Machine Learning Methods

Machine-learning models were developed using Python (version 3.8.10). The samples from the discovery and derivation cohorts were divided into a 70% training set (62 samples) and 30% test set (26 samples). The test set was exclusively used to evaluate the model performance and remained hidden during training. We utilized Random Forest (RF), Support Vector Machine (SVM), and Extreme Gradient Boosting (XGBoost) algorithms to ensure a balanced patient-to-control ratio and to avoid data imbalance affecting model generalization.

To prevent overfitting, we employed random dataset shuffling and performed 100 iterations with the receiver operating characteristic area under the curve (ROC-AUC) scores calculated for each. The average area under the curve (AUC) served as the performance metric, and accuracy and recall were computed. Learning curves were used to detect overfitting, and a 95% confidence interval (CI) was calculated using five-fold cross validation. If the testing set AUCs fell within the 95% CI of the training set AUCs, the model was not considered overfitted.[33] The best performing model among RF, SVM, and XGBoost was selected as the final diagnostic model.

Correlation Analysis Between Biomarkers and Clinical Data

To further demonstrate the relationship between these biomarkers and existing clinical indicators, we performed the correlation analysis between them in our cohorts. The pairwise Pearson correlation test was used, and the Circos plot was drawn according to the correlation coefficient and P-value using the circular package (version 0.4.10) in R.

ELISA Assay

Seven DEPs were identified as candidate biomarkers and tested by ELISA using 80 serum samples from the validation cohort. All ELISA kits were purchased from RayBiotech Life. Experiments were performed in accordance with the manufacturer's instructions. The signal from each well was read at 450 nm immediately after the ELISA. The absolute quantitation levels of the biomarkers were determined using the standard curves for each ELISA plate. The final concentrations of biomarkers were calculated based on the dilution ratio.

Statistics Analysis

SPSS (version 22.0), GraphPad Prism (version 8.0.0), and R software were used for data analysis. The baseline characteristics were collected for all participants without missing data. Categorical variables are presented as numbers (n) and percentages (%). Continuous variables with normal distributions are presented as means and standard deviations (SD), and those with abnormal distributions are presented as medians and interquartile ranges (IQR). The Shapiro–Wilk test was used to check for normal distribution. Data passing the normality test were subjected to unpaired t-tests for statistical analysis and Fisher's test to compare variances. Non-normal data were analyzed using the Mann–Whitney U-test. Statistical significance was set at P value < 0.05. Binary multivariable logistic regression was used to select clinical indicators with a significant difference (P < 0.0001) between patients with TBAD and healthy controls. The accuracy, recall, precision, F1 score, and AUC of the machine-learning models were assessed using ROC analysis.

Results

Screening Out Thirty-One DEPs Among 1000 Serum Proteins in Discovery Cohort

The workflow for screening serum DEPs in the discovery cohort is shown in Figure 2a. Proteomic analysis examined eight serum samples from five patients with TBAD and three healthy controls, and identified 67 DEPs out of 1000 serum proteins (Figure 2b, Supplemental Figure 1a and b). The heatmap (Figure 2c) showed 12 upregulated and 55 down-regulated proteins. Using the KEGG database, we found significant enrichment of these DEPs in 11 pathways (adjusted P-value < 0.05), including cytokine-cytokine receptor interactions, cell adhesion molecules (CAMs), and natural killer cell-mediated cytotoxicity, suggesting their importance in TBAD pathogenesis.

Functional and regulatory interactions among the 67 DEPs were analyzed using a PPI network based on the STRING database (Figure 2d). The top 50% altered proteins were selected for verification, excluding 2B4 (CD244) and TRAIL from the analysis because of their co-expression with CD229 (Lymphocyte Antigen 9, LY9) and TRAILR4. Finally, 31 DEPs were identified for verification.
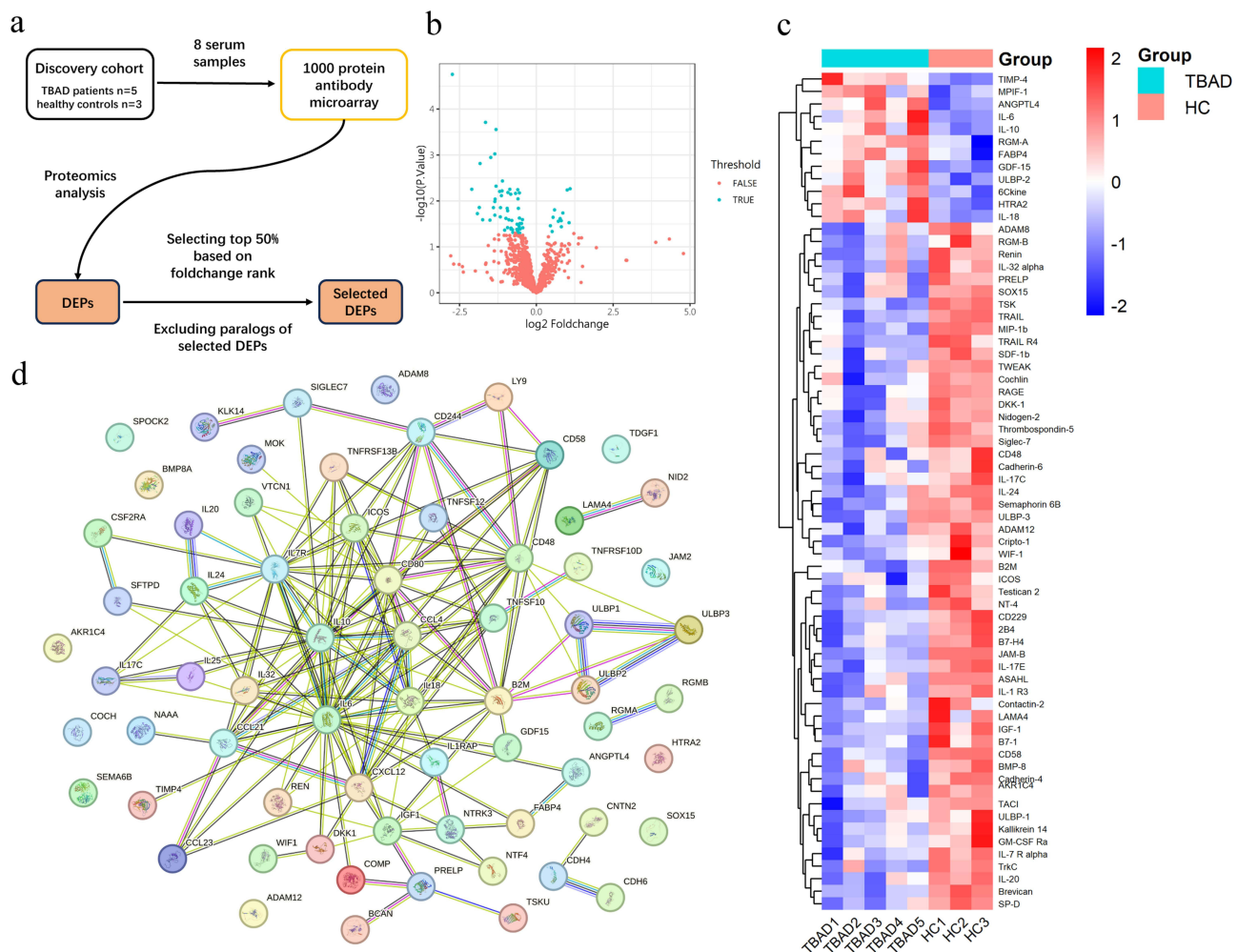
Figure 2 Screening serum DEPs through proteomics profiling in discovery cohort. (**a**) The workflow of screening DEPs between patients with TBAD and healthy controls in discovery cohort. (**b**) Volcano plot shows 67 DEPs are screened out from 1000 serum proteins in discovery cohort and depicted in blue. (**c**) Heatmap of the 1000 protein arrays screening 67 DEPs (fold change > 1.2 and P < 0.05) using serum samples from patients with TBAD (n = 5) and healthy controls (n = 3). DEPs were identified through a moderated t-statistic and were adjusted using the Benjamini-Hochberg method to control for false discovery rates. (**d**) Protein-protein interaction (PPI) network among the 67 DEPs was established using the STRING database. Each node is a DEP containing a 3D protein structure inside. The node color represents the predicted functional associations: black, co-expression evidence; yellow, text-mining evidence; blue, sequence similarity evidence; purple, experimental evidence.

Verifying Eleven DEPs Using Customized Antibody Microarray in Derivation Cohort

In a derivation cohort of 50 patients with TBAD and 30 healthy controls, 31 serum proteins were analyzed using RayBio® Custom Human Antibody Arrays in 80 serum samples. The workflow used to verify the selected DEPs is shown in Figure 3a. Comparative analysis identified 11 DEPs with significant differences in expression: four were upregulated (IL6, IL10, GDF-15, CCL23) and seven were downregulated (LY9, Siglec-7, CD58, KLK14, CDH4, CDH6, and SFTPD) in patients with TBAD
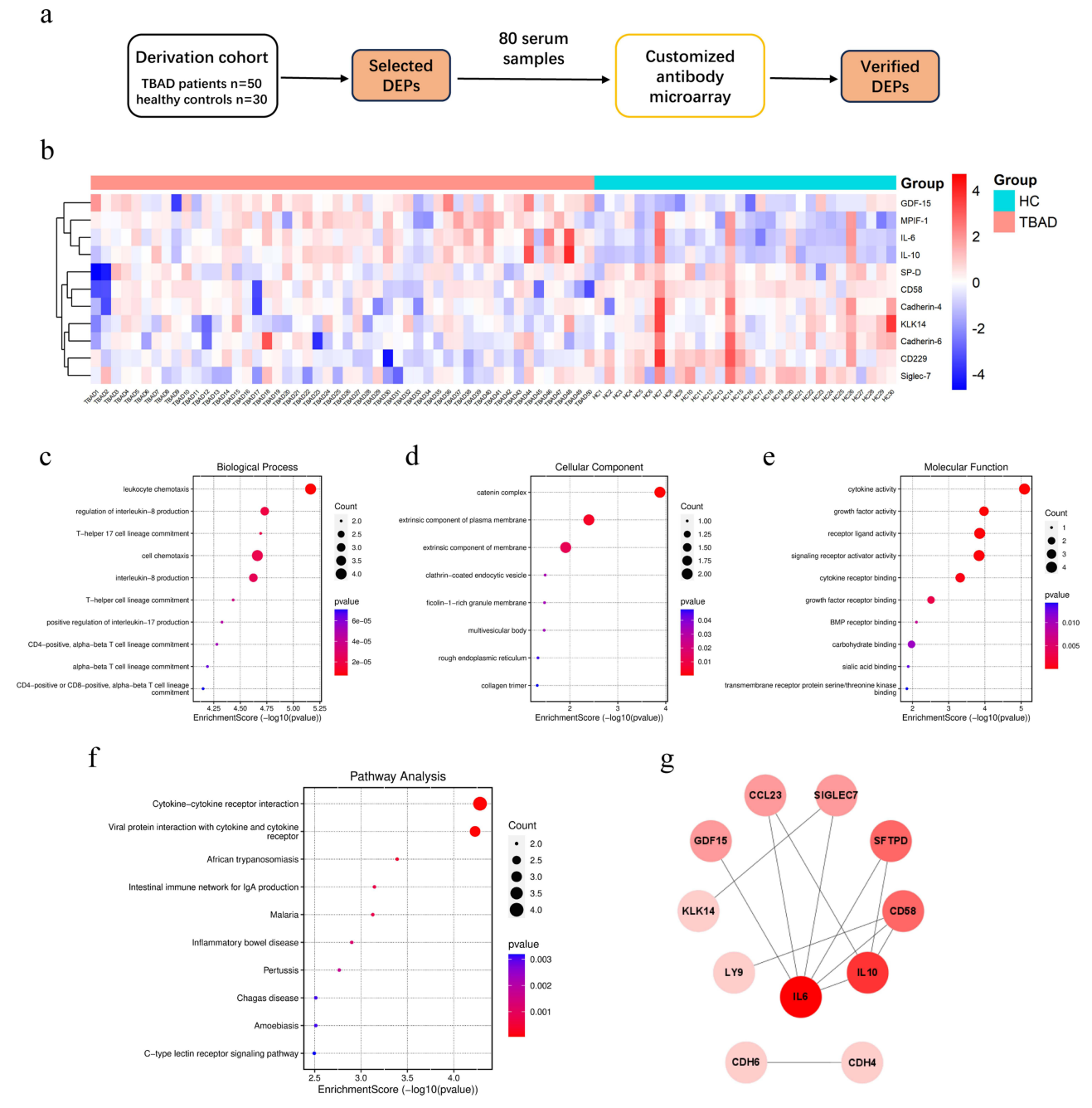

Figure 3 Further verifying selected serum DEPs using customized antibody microarray in derivation cohort. (**a**) The workflow of verifying selected DEPs through customized antibody microarray in derivation cohort. (**b**) Heatmap of the customized arrays verifying 11 DEPs from 31 DEPs in the derivation cohort comprising 50 patients with TBAD and 30 healthy controls. MPIF-1: CCL23, SP-D: SFTPD, Cadherin-4: CDH4, Cadherin-6: CDH6, CD229: LY9. (**c**) Biological process analysis of 11 DEPs based on GO annotations. The enrichment score is -log10 (P value) of each GO term. The dot size represents the number of DEPs, while colors correspond to the P value range. (**d**) Cellular component analysis of 11 DEPs based on GO annotations. The enrichment score is -log10 (P value) of each GO term. The dot size represents the number of DEPs, while colors correspond to the P value range. (**e**) Molecular function analysis of 11 DEPs based on GO annotations. The enrichment score is -log10 (P value) of each GO term. The dot size represents the number of DEPs, while colors correspond to the P value range. (**f**) KEGG pathway analysis of 11 DEPs in TBAD. The enrichment score is -log10 (P value) of each pathway. The dot size represents the number of DEPs, while colors correspond to the P value range. (**g**) Hub gene analysis of 11 DEPs. IL-6 is recognized as the hub gene according to MCC scores from Cyto-Hubba.

 539

(Figure 3b, Supplemental Figure 1c and d). Enrichment analysis using the GO database (Figure 3c–3e) highlighted processes, such as leukocyte chemotaxis and cytokine-cytokine receptor interaction, suggesting that the potential pathological mechanisms of TBAD involve immune cell chemotaxis and cytokine-mediated processes. The KEGG pathway analysis further supported these findings. Additionally, PPI analysis using STRING identified IL6 and IL10 as the top hub genes, indicating their central roles in TBAD pathology (Figure 3g).

Discovering Six Candidate Biomarkers Through Optimal Machine Learning Algorithms

We employed three machine learning algorithms, (RF), XGBoost, and Support Vector Machine (SVM), to develop TBAD diagnostic models and identify serum biomarkers (Figure 4a). The RF model with an AUC of 0.904±0.06, based on 11 DEPs, outperformed XGBoost and SVM in distinguishing patients with TBAD from healthy controls (Figure 4b and Table S2). The learning curves confirmed the robustness of the RF model without overfitting (Supplementary Figure 2a). Thus, RF was selected as a definitive diagnostic model for TBAD.

To analyze the feature importance of RF for TBAD biomarker identification, we ranked the Gini values of the 11 DEPs. Those with Gini values above 0.1 were considered as potential TBAD serum biomarkers. This led to the selection of 6 DEPs (IL-6, IL-10, Siglec-7, GDF-15, LY9, and CD58), excluding the other 5 (Figure 4c, Supplemental Figure 2b). A refined RF model with these six DEPs exhibited efficacy (AUC=0.875±0.06) comparable to that of the original 11-DEP model (Figure 4d). Both models showed similar accuracy metrics (Figure 4e), indicating that these six DEPs are crucial for RF model prediction and effective for TBAD diagnosis.
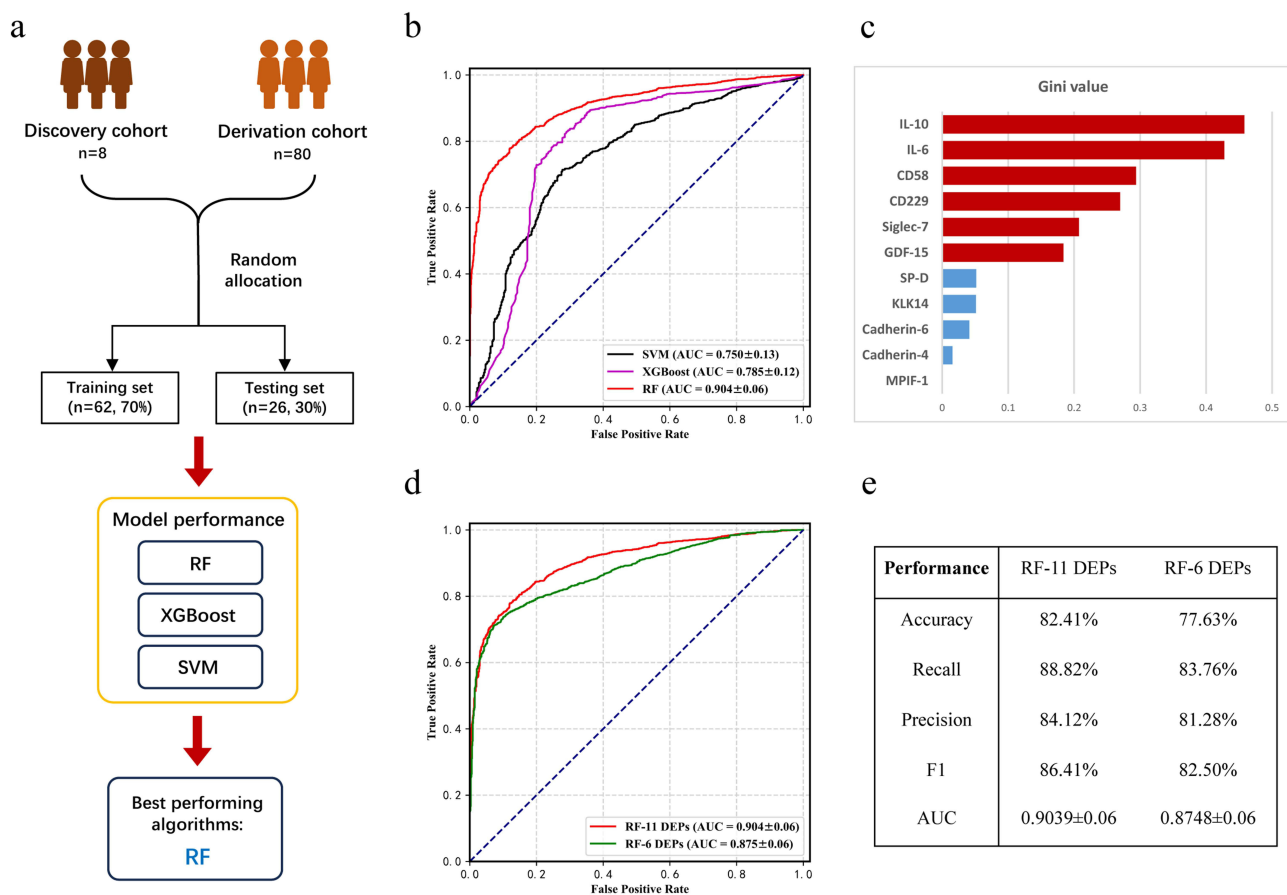

Figure 4 Optimal machine learning algorithm was confirmed to further screen biomarkers. (**a** and **b**) Comparing performances of three algorithms (Random Forest (RF), Support Vector Machine (SVM) and Extreme Gradient Boosting (XGBoost)) through ROC analysis. 88 participants from discovery and derivation cohort were randomly allocated into training set (62 participants, accounting for 70%) and testing set (26 participants, accounting for 30%). (**c**) Gini value rank of all eleven DEPs in the RF model. MPIF-1: CCL23, SP-D: SFTPD, Cadherin-4: CDH4, Cadherin-6: CDH6, CD229: LY9. (**d** and **e**) Comparing the performance of two RF models (eleven DEPs versus six DEPs). Eleven DEPs include IL6, IL10, GDF-15, CCL23, LY9, Siglec-7, CD58, KLK14, CDH4, CDH6 and SFTPD; Six DEPs include IL-6, IL-10, Siglec-7, GDF-15, LY9 and CD58.

External Validation of Candidate Biomarkers Using ELISA in an Independent Cohort

To validate the six candidate TBAD biomarkers, we used an independent cohort of 50 patients with TBAD and 30 healthy controls. Absolute-quantitation ELISA revealed significant increases in GDF-15 and IL-6 levels in patients with TBAD ($P < 0.05$). Conversely, CD58, LY9, and Siglec-7 levels were decreased in patients with TBAD ($P < 0.05$), consistent with the initial proteomic profiling (Figure 5a–5e). IL-10 showed no significant classification capability in TBAD (Figure 5f). We developed two RF models: one with all six biomarkers, and the other excluding IL-10. The 5-biomarker model's accuracy was comparable to the 6-biomarker model in both proteomics and ELISA (AUC = 0.865±0.06 and AUC = 0.866±0.06, respectively) (Figure 5g–5h). These results validate GDF-15, IL-6, CD58, LY9, and Siglec-7 as effective TBAD serum biomarkers suitable for both relative and absolute quantitative analyses.
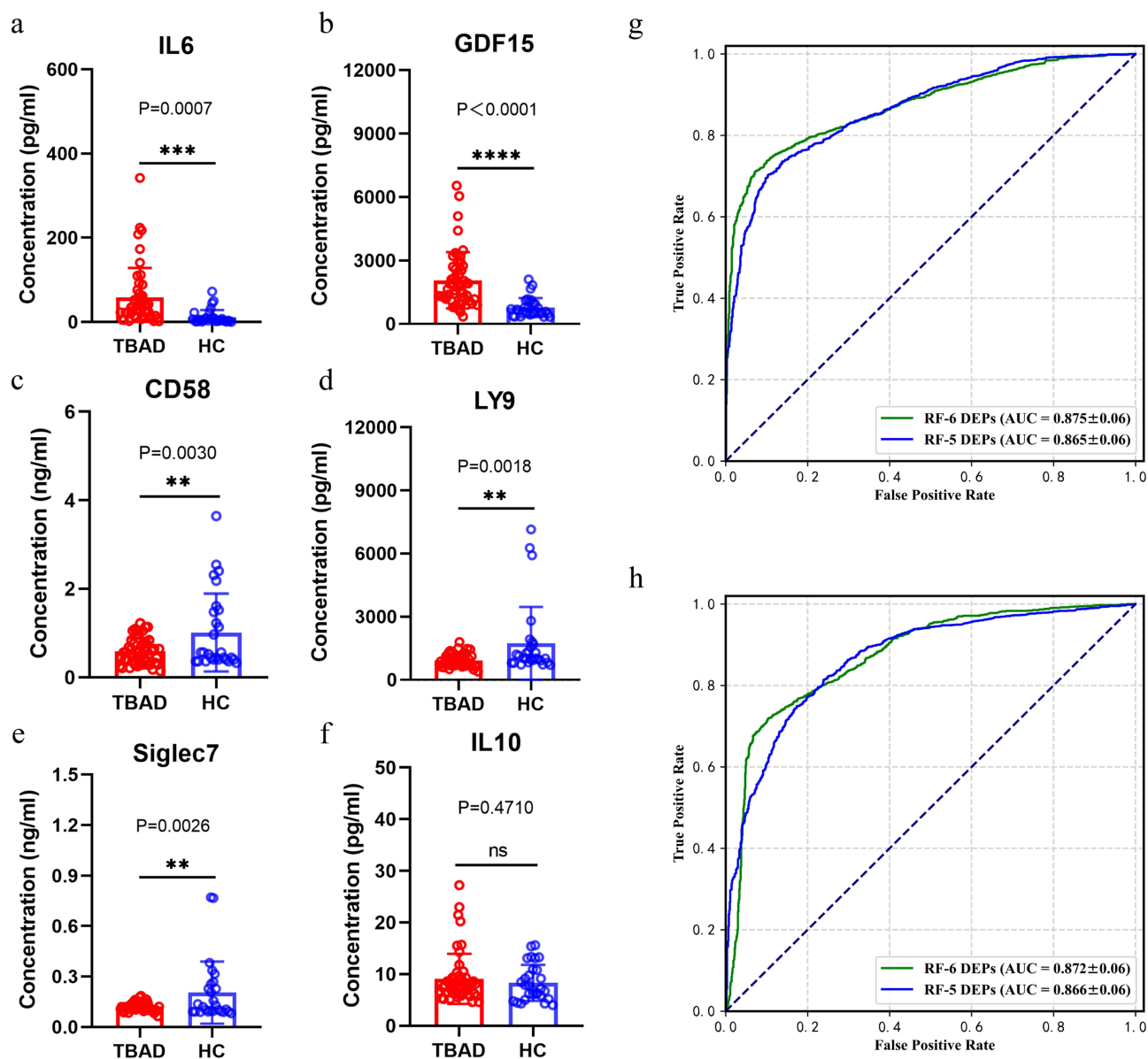
Figure 5 Validation of candidate biomarkers using ELISA in an independent cohort. (**a–f**) Expression levels of candidate biomarkers in serum samples from the validation cohort by ELISA assays. (**g**) Comparing the performance of two RF models (5 DEPs versus 6 DEPs) using proteomics profiling with relative quantitation in discovery and derivation cohort. (**h**) Comparing the performance of two RF models (5 DEPs versus 6 DEPs) using ELISA with absolute quantitation in validation cohort. Data are presented as mean ± SD. **$P < 0.01$, ***$P < 0.001$, and ****$P < 0.0001$ by unpaired Student's t-test.

Establishment of Combined Model Incorporating TBAD Biomarkers and Selected Clinical Indicators

To enhance TBAD diagnosis, we integrated the clinical data with the identified biomarkers using the RF algorithm (Figure 6a). We gathered comprehensive blood indicators from 168 participants, including various blood cell counts, hemoglobin concentrations, and cholesterol levels, as detailed in Table S1. Binary multivariable logistic regression revealed significant differences in the blood indicators between patients with TBAD and healthy controls ($p < 0.0001$) (Figure 6b). Correlation analysis was used to examine the interactions between these biomarkers and blood indicators in TBAD, visualized in circus plots (Figure 6c–6f).

Proteomic profiling and ELISA assays across three Chinese cohorts identified five serum biomarkers and recorded ten blood-related blood indicators for 168 participants. Using the RF algorithm, we developed diagnostic models that integrate these biomarkers and blood indicators for TBAD classification. The models showed substantial effectiveness, with AUC values of 0.865, 0.904, and 0.909, respectively (Figure 6g and Table S3). The absolute quantitation ELISA also performed well (AUC values of 0.866, 0.868, and 0.886, as shown in Figure 6h and Table S4). Notably, the combined models outperformed individual biomarkers and clinical models, confirming the diagnostic efficacy of TBAD. The learning curves indicated no overfitting (Supplemental Figure 3), thus validating these models as effective diagnostic tools for TBAD. Hypertension is a strong risk factor of TBAD. Identifying potential patients in the hypertensive population is crucial for the early warning of TBAD. We also evaluated the performance of our models in hypertensive participants. The AUC values of the biomarkers, clinical, and combined models were 0.853, 0.894, and 0.925, respectively, in the discovery and derivation cohorts (Supplemental Figure 4 and Table S5). These results were verified in the validation cohort (AUC values of 0.857, 0.838, and 0.904, respectively, as shown in Supplemental Figure 5 and Table S6). The results demonstrated that diagnostic models could also be applied to the hypertensive population to diagnose TBAD.

Discussion

To address the diagnostic challenges of TBAD during routine health checkups, this study used circulating protein profiling arrays and machine learning to identify TBAD biomarkers. Our extensive serum protein screening via proteomics has identified GDF-15, IL-6, CD58, LY9, and Siglec-7 as potential TBAD biomarkers. A machine learning model integrating these biomarkers with blood indicators demonstrated superior accuracy in diagnosing TBAD. This study is the first investigation of serum TBAD biomarkers in Chinese cohorts. In addition, this is an inaugural study to develop an effective diagnostic model for TBAD based on blood samples.

Biomarkers exhibit a powerful ability in the screening, diagnosis and monitoring of cardiovascular diseases. With the development of detective techniques, such as nanoparticle biosensors and spectroscopy,[34,35] the availability and accessibility of biomarker detection have been facilitated currently. Serum is ideal for biomarker discovery due to its accessibility and biological content.[12] Previous studies have identified serum biomarkers of aortic dissection, including smooth muscle markers, and others.[13] Discovered serum biomarkers of aortic dissection include serum succinate, soluble ST2, and ceruloplasmin.[15,16,36] Some studies have suggested the diagnostic potential of serum tenascin-C, VE-cadherin, and vinculin levels, nevertheless requiring further validation.[37,38] Profiling a wide range of serum proteins offers unbiased marker discovery, enhances diagnostic accuracy, and provides insights into pathophysiology and therapeutic targets.[20] Advances in proteomics, particularly high-throughput techniques such as mass spectrometry and antibody microarrays, have revolutionized biomarker identification.[39,40] Antibody microarrays are cost-effective and efficient, excel at screening lower-abundance serum proteins.[40,41] In our study, we used antibody microarrays to screen TBAD biomarkers among 1000 serum proteins, bringing new insights into TBAD pathogenesis.

Machine learning has transformed disease understanding through omics data analysis.[26,42] Proteomics-driven machine learning has effectively assisted biomarker discovery, risk stratification, and prognosis evaluation in various fields.[43–48] Our study uniquely combined antibody microarrays with machine learning to identify TBAD biomarkers and to develop diagnostic models. We assessed several algorithms such as RF, SVM, and XGBoost, with RF proving superior in terms of its robustness and data resilience.[49,50] The RF models in our study exhibited high accuracy with minimal tuning. By
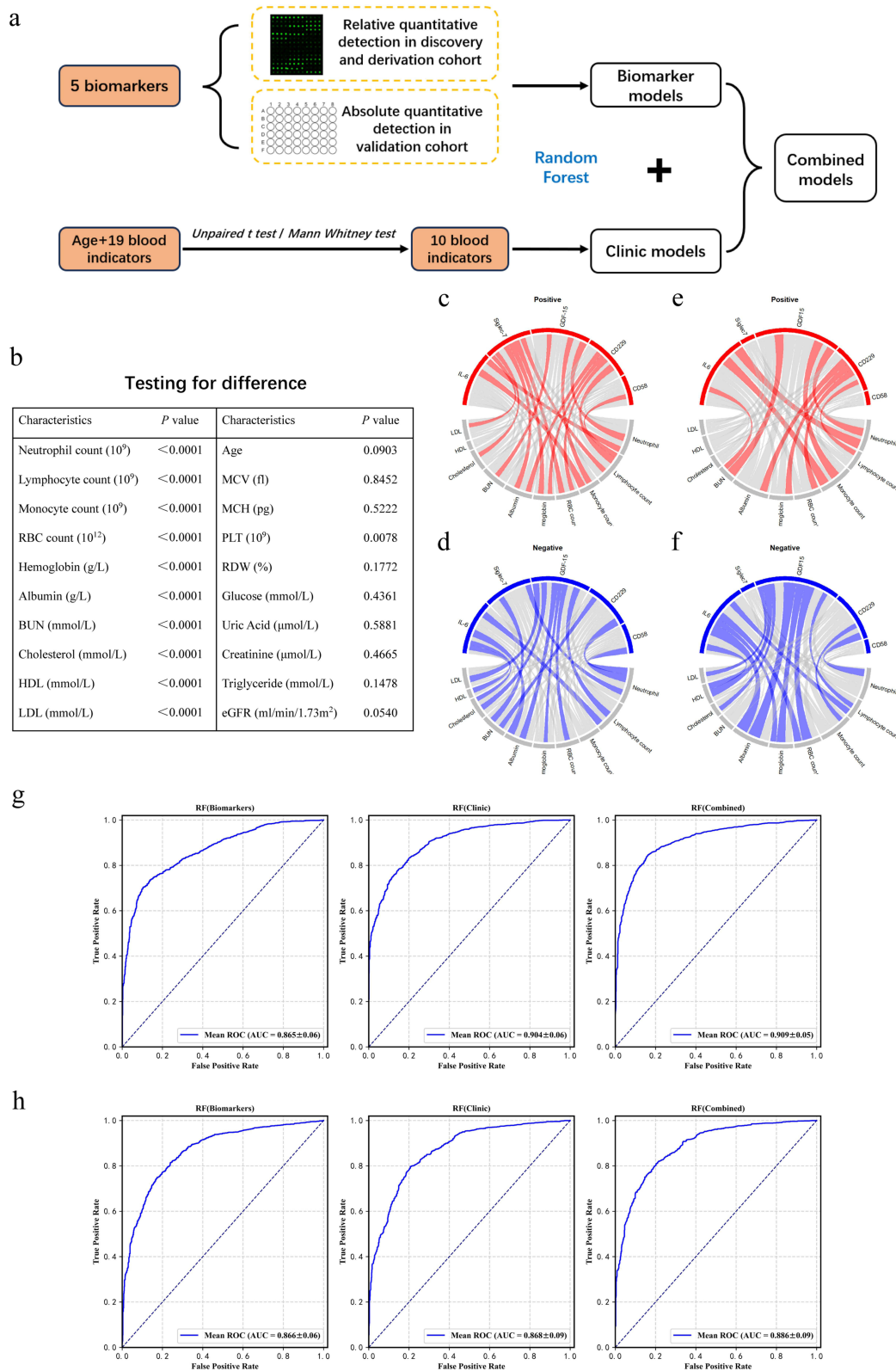
Figure 6 Establishment of combined model incorporating biomarkers and clinical indicators. (**a**) The strategy on combined model establishment. (**b**) Testing for difference of age and 19 blood indicators. Binary multivariable logistic regression was used for selecting indicators with vital statistical difference (P value < 0.0001) between patients with TBAD and healthy controls. (**c** and **d**) Correlation network of biomarkers (using relative quantitative detection) and clinical indicators in discovery cohort and derivation cohort. Positive correlation with statistical significance (P value <0.05) is indicated in red. Negative correlation with statistical significance (P value <0.05) is indicated in blue. Correlation without statistical significance (P value ≥0.05) is indicated in gray. (**e** and **f**) Correlation network of biomarkers (using absolute quantitative detection) and clinical indicators in validation cohort. MPIF-1: CCL23, SP-D: SFTPD, Cadherin-4: CDH4, Cadherin-6: CDH6, CD229: LY9. (**g**) Combined model performance with biomarkers (using relative quantitative detection) and 10 clinical indicators. (**h**) Combined model performance with biomarkers (using absolute quantitative detection) and 10 clinical indicators.

integrating clinical blood indicators with biomarkers, our model surpassed those based on clinical blood indicators or biomarkers alone, thereby enhancing the TBAD diagnosis and the understanding of pathogenesis.[45,47,48]

The general pathological mechanisms of aortic dissection include smooth muscle cell injury, elastic fiber degradation, and inflammatory cell infiltration, which lead to a weakened aortic wall and the formation of dissection.[51] Multiple cytokines contribute to the pathogenesis of aortic dissection, including interleukins, chemokines, tumor necrosis factor superfamily, growth factors, and so on.[52] Our study identified five serum proteins among cytokines as biomarkers linked to TBAD: IL-6, GDF-15, CD58, LY9, and Siglec-7. IL-6 induces inflammatory, oxidative, and fibrotic responses[53–55] and is associated with aortic dissection.[56] As a crucial inflammatory cytokine, IL-6 affects recruitment, functional activation, differentiation, and infiltration of immune cells.[57] Elevated IL-6 levels lead to increased inflammation and mediates aortic dissection,[58,59] implicating it in TBAD pathogenesis. GDF-15 is a member of the TGF-β superfamily that exerts anti-inflammatory effects in many metabolic diseases.[60] GDF-15 is associated with abdominal aortic aneurysms and stenosis.[61,62] Increased levels of GDF-15 have been observed in patients with TBAD; however, the underlying mechanisms are not fully understood. CD58, also known as lymphocyte function antigen 3 (LFA-3), is broadly expressed in tissue cells. CD58 plays a crucial role in NK cell activation and proliferation by interacting with CD2.[63] Siglec-7, which belongs to the Siglec receptors family, is an MHC class I-independent inhibitory receptor of T/NK cells.[64–66] Both CD58 and Siglec-7 are associated with T/NK cells, which are cytotoxic immune cells in the peripheral blood, suggesting a vital role of immune-mediated cytotoxicity in TBAD progression. Lymphocyte Antigen 9 (LY9), also known as CD229, is expressed on B and T lymphocytes, and influences their development and function.[67,68] However, the relationship between LY9 expression and aortic dissection remains unclear. Our findings revealed decreased levels of CD58, LY9, and Siglec-7 in the TBAD cohort, indicating significant involvement of immune responses, particularly T/NK cells, in TBAD pathogenesis.

Our model provides a noninvasive, radiation-free tool for diagnosing TBAD during routine health checkups. The RF model, which integrates biomarkers and clinical blood indicators, offers a convenient method that uses only blood samples to avoid the risks of radiation and contrast agents. In particular, our models are applicable to a hypertensive population, contributing to the precise diagnosis of TBAD. This method improves early stage TBAD detection and treatment decision-making.

Our study has several limitations. First, the sample size was limited due to the low incidence of TBAD. Further study, including an expanded and larger sample size, should be conducted. Secondly, the specificity of the identified biomarkers requires further validation to distinguish TBAD from other diseases. Third, we did not analyze biomarker expression in the aortic tissue as almost all TBAD patients undergo endovascular rather than open surgery, limiting tissue sample availability. Fourth, limitations in detection accuracy may have missed some biomarkers. Finally, as the study focused on a Chinese population, a broader ethnic validation is needed. Future research should include larger, multicenter studies to enhance the generalizability of our findings.

Conclusion

Serum IL-6, GDF-15, CD58, LY9, and Siglec-7 levels have been identified and validated as TBAD biomarkers. Our RF model, integrating these five biomarkers with 10 clinical indicators, demonstrated high accuracy in TBAD prediction. The proteomic profiling-enabled machine learning model exhibited a significant potential for TBAD diagnosis within a population.

Data Sharing Statement

All data generated in the research were available from Prof. Zhao Liu and could be provided if necessary.

Ethics Approval and Informed Consent

This study was approved by the ethics committee of Nanjing Drum Tower Hospital, affiliated with Nanjing University Medical School (Approval number: 2022-678). The study adhered to relevant regulations regarding human participants and was conducted in accordance with the Declaration of Helsinki. Informed consent was obtained from all participants to ensure full understanding and agreement.

Acknowledgments

Author Contributions

All authors made a significant contribution to the work reported, whether that is in the conception, study design, execution, acquisition of data, analysis and interpretation, or in all these areas; took part in drafting, revising or critically reviewing the article; gave final approval of the version to be published; have agreed on the journal to which the article has been submitted; and agree to be accountable for all aspects of the work.

Funding

Disclosure

The author(s) report no conflicts of interest in this work.

References

1. Hughes GC, Andersen ND, McCann RL. Management of acute type B aortic dissection. *J Thorac Cardiovasc Surg*. 2013;145(3 Suppl):S202–7. doi:10.1016/j.jtcvs.2012.11.078
2. Tadros RO, Tang GHL, Barnes HJ, et al. Optimal Treatment of Uncomplicated Type B Aortic Dissection. *J Am Coll Cardiol*. 2019;74 (11):1494–1504. doi:10.1016/j.jacc.2019.07.063
3. Lombardi JV, Hughes GC, Appoo JJ, et al. Society for Vascular Surgery (SVS) and Society of Thoracic Surgeons (STS) reporting standards for type B aortic dissections. *J Vasc Surg*. 2020;71(3):723–747. doi:10.1016/j.jvs.2019.11.013
4. Gouveia EMR, Mourão M, Caldeira D, et al. A systematic review and meta-analysis of the incidence of acute aortic dissections in population-based studies. *J Vasc Surg*. 2022;75(2):709–720. doi:10.1016/j.jvs.2021.08.080
5. Pape LA, Awais M, Woznicki EM, et al. Presentation, Diagnosis, and Outcomes of Acute Aortic Dissection: 17-Year Trends From the International Registry of Acute Aortic Dissection. *J Am Coll Cardiol*. 2015;66(4):350–358. doi:10.1016/j.jacc.2015.05.029
6. Howard DP, Sideso E, Handa A, Rothwell PM. Incidence, risk factors, outcome and projected future burden of acute aortic dissection. *Ann Cardiothorac Surg*. 2014;3(3):278–284. doi:10.3978/j.issn.2225-319X.2014.05.14
7. Erbel R, Aboyans V, Boileau C, et al. ESC Guidelines on the diagnosis and treatment of aortic diseases: document covering acute and chronic aortic diseases of the thoracic and abdominal aorta of the adult. The Task Force for the Diagnosis and Treatment of Aortic Diseases of the European Society of Cardiology (ESC). *Eur Heart J*. 2014;35(41):2873–2926. doi:10.1093/eurheartj/ehu281
8. Bossone E, Eagle KA. Epidemiology and management of aortic disease: aortic aneurysms and acute aortic syndromes. *Nat Rev Cardiol*. 2021;18 (5):331–348. doi:10.1038/s41569-020-00472-6
9. Nienaber CA, Clough RE. Management of acute aortic dissection. *Lancet*. 2015;385(9970):800–811. doi:10.1016/s0140-6736(14)61005-9
10. Chen H, Li Y, Li Z, Shi Y, Zhu H. Diagnostic biomarkers and aortic dissection: a systematic review and meta-analysis. *BMC Cardiovasc Disord*. 2023;23(1):497. doi:10.1186/s12872-023-03448-9
11. Ranasinghe AM, Bonser RS. Biomarkers in acute aortic dissection and other aortic syndromes. *J Am Coll Cardiol*. 2010;56(19):1535–1541. doi:10.1016/j.jacc.2010.01.076
12. Keshishian H, Burgess MW, Specht H, et al. Quantitative, multiplexed workflow for deep analysis of human blood plasma and biomarker discovery by mass spectrometry. *Nat Protoc*. 2017;12(8):1683–1701. doi:10.1038/nprot.2017.054
13. Nienaber CA, Clough RE, Sakalihasan N, et al. Aortic dissection. *Nat Rev Dis Primers*. 2016;2(1):16053. doi:10.1038/nrdp.2016.53
14. Pietzner M, Wheeler E, Carrasco-Zanini J, et al. Mapping the proteo-genomic convergence of human diseases. *Science*. 2021;374(6569):eabj1541. doi:10.1126/science.abj1541
15. Wang Y, Tan X, Gao H, et al. Magnitude of Soluble ST2 as a Novel Biomarker for Acute Aortic Dissection. *Circulation*. 2018;137(3):259–269. doi:10.1161/circulationaha.117.030469
16. Cui H, Chen Y, Li K, et al. Untargeted metabolomics identifies succinate as a biomarker and therapeutic target in aortic aneurysm and dissection. *Eur Heart J*. 2021;42(42):4373–4385. doi:10.1093/eurheartj/ehab605
17. Zhou X, Wang R, Zhang T, et al. Identification of Lysophosphatidylcholines and Sphingolipids as Potential Biomarkers for Acute Aortic Dissection via Serum Metabolomics. *Eur J Vasc Endovasc Surg*. 2019;57(3):434–441. doi:10.1016/j.ejvs.2018.07.004
18. Adamcova M, Šimko F. Multiplex biomarker approach to cardiovascular diseases. *Acta Pharmacol Sin*. 2018;39(7):1068–1072. doi:10.1038/aps.2018.29

19. Curry SJ, Krist AH, Owens DK, et al. Risk Assessment for Cardiovascular Disease With Nontraditional Risk Factors: US Preventive Services Task Force Recommendation Statement. *JAMA*. 2018;320(3):272–280. doi:10.1001/jama.2018.8359

20. Smith JG, Gerszten RE. Emerging Affinity-Based Proteomic Technologies for Large-Scale Plasma Profiling in Cardiovascular Disease. *Circulation*. 2017;135(17):1651–1664. doi:10.1161/circulationaha.116.025446

21. Rylski B, Schilling O, Czerny M. Acute aortic dissection: evidence, uncertainties, and future therapies. *Eur Heart J*. 2023;44(10):813–821. doi:10.1093/eurheartj/ehac757

22. Coussot G, Le Postollec A, Faye C, et al. Photochemistry on the Space Station-Antibody Resistance to Space Conditions after Exposure Outside the International Space Station. *Astrobiology*. 2019;19(8):1053–1062. doi:10.1089/ast.2018.1907

23. Ren AH, Diamandis EP, Kulasingam V. Uncovering the Depths of the Human Proteome: antibody-based Technologies for Ultrasensitive Multiplexed Protein Detection and Quantification. *Mol Cell Proteomics*. 2021;20:100155. doi:10.1016/j.mcpro.2021.100155

24. Cheng L, Wang D, Wang Z, et al. Proteomics Landscape Mapping of Organ-Resolved Behçet's Disease Using In-Depth Plasma Proteomics for Identifying Hyaluronic Binding Protein 2 Expression Associated With Vascular Involvement. *Arthritis Rheumatol*. 2023;75(3):424–437. doi:10.1002/art.42348

25. Peiffer-Smadja N, Rawson TM, Ahmad R, et al. Machine learning for clinical decision support in infectious diseases: a narrative review of current applications. *Clin Microbiol Infect*. 2020;26(5):584–595. doi:10.1016/j.cmi.2019.09.009

26. Reel PS, Reel S, Pearson E, Trucco E, Jefferson E. Using machine learning approaches for multi-omics data analysis: a review. *Biotechnol Adv*. 2021;49:107739. doi:10.1016/j.biotechadv.2021.107739

27. Handelman GS, Kok HK, Chandra RV, Razavi AH, Lee MJ, Asadi H. eDoctor: machine learning and the future of medicine. *J Intern Med*. 2018;284(6):603–619. doi:10.1111/joim.12822

28. Niu L, Thiele M, Geyer PE, et al. Noninvasive proteomic biomarkers for alcohol-related liver disease. *Nat Med*. 2022;28(6):1277–1287. doi:10.1038/s41591-022-01850-y

29. Karayel O, Virreira Winter S, Padmanabhan S, et al. Proteome profiling of cerebrospinal fluid reveals biomarker candidates for Parkinson's disease. *Cell Rep Med*. 2022;3(6):100661. doi:10.1016/j.xcrm.2022.100661

30. Poss AM, Maschek JA, Cox JE, et al. Machine learning reveals serum sphingolipids as cholesterol-independent biomarkers of coronary artery disease. *J Clin Invest*. 2020;130(3):1363–1376. doi:10.1172/jci131838

31. Bowman WS, Newton CA, Linderholm AL, et al. Proteomic biomarkers of progressive fibrosing interstitial lung disease: a multicentre cohort analysis. *Lancet Respir Med*. 2022;10(6):593–602. doi:10.1016/s2213-2600(21)00503-8

32. Ni J, Chen C, Wang S, et al. Novel CSF biomarkers for diagnosis and integrated analysis of neuropsychiatric systemic lupus erythematosus: based on antibody profiling. *Arthritis Res Ther*. 2023;25(1):165. doi:10.1186/s13075-023-03146-z

33. Baturynska I, Martinsen K. Prediction of geometry deviations in additive manufactured parts: comparison of linear regression with machine learning algorithms. *Journal of Intelligent Manufacturing*. 2021;32(1):179–200. doi:10.1007/s10845-020-01567-0

34. Saadh MJ, Muhammad FA, Albadr RJ, et al. Nanoparticle biosensors for cardiovascular disease detection. *Clin Chim Acta*. 2024;567:120094. doi:10.1016/j.cca.2024.120094

35. Buchan E, Harbi MH, Rickard JJS, Thomas M, Goldberg Oppenheimer P. Advanced biomolecular spectroscopic profiling of cardiovascular disease macromolecular markers: SIL-6, IL-9, LpA, ApoB, PCSK9 and NT-ProBNP for rapid in-situ detection and monitoring. *Int J Biol Macromol*. 2024;284(Pt 1):138115. doi:10.1016/j.ijbiomac.2024.138115

36. Ma C, Zhao H, Shi F, et al. Serum Ceruloplasmin Is the Candidate Predictive Biomarker for Acute Aortic Dissection and Is Related to Thrombosed False Lumen: a Propensity Score-Matched Observational Case-Control Study. *Biol Trace Elem Res*. 2021;199(3):895–911. doi:10.1007/s12011-020-02219-3

37. Nozato T, Sato A, Hirose S, et al. Preliminary study of serum tenascin-C levels as a diagnostic or prognostic biomarker of type B acute aortic dissection. *Int J Cardiol*. 2013;168(4):4267–4269. doi:10.1016/j.ijcard.2013.04.211

38. Wang S, Li X, Jiang H, Zhang J. High Serum VE-Cadherin and Vinculin Concentrations Are Markers of the Disruption of Vascular Integrity during Type B Acute Aortic Dissection. *J Clin Med*. 2023;12(14):4730. doi:10.3390/jcm12144730

39. Geyer PE, Voytik E, Treit PV, et al. Plasma Proteome Profiling to detect and avoid sample-related biases in biomarker studies. *EMBO Mol Med*. 2019;11(11):e10427. doi:10.15252/emmm.201910427

40. Han B, Li C, Li H, et al. Discovery of plasma biomarkers with data-independent acquisition mass spectrometry and antibody microarray for diagnosis and risk stratification of pulmonary embolism. *J Thromb Haemost*. 2021;19(7):1738–1751. doi:10.1111/jth.15324

41. Huang R, Jiang W, Yang J, et al. A biotin label-based antibody array for high-content profiling of protein expression. *Cancer Genomics Proteomics*. 2010;7(3):129–141.

42. Li R, Li L, Xu Y, Yang J. Machine learning meets omics: applications and perspectives. *Brief Bioinform*. 2022;23(1). doi:10.1093/bib/bbab460

43. Bauer Y, de Bernard S, Hickey P, et al. Identifying early pulmonary arterial hypertension biomarkers in systemic sclerosis: machine learning on proteomics from the DETECT cohort. *Eur Respir J*. 2021;57(6):2002591. doi:10.1183/13993003.02591-2020

44. Chirinos JA, Orlenko A, Zhao L, et al. Multiple Plasma Biomarkers for Risk Stratification in Patients With Heart Failure and Preserved Ejection Fraction. *J Am Coll Cardiol*. 2020;75(11):1281–1295. doi:10.1016/j.jacc.2019.12.069

45. Bom MJ, Levin E, Driessen RS, et al. Predictive value of targeted proteomics for coronary plaque morphology in patients with suspected coronary artery disease. *EBioMedicine*. 2019;39:109–117. doi:10.1016/j.ebiom.2018.12.033

46. Unterhuber M, Kresoja KP, Rommel KP, et al. Proteomics-Enabled Deep Learning Machine Algorithms Can Enhance Prediction of Mortality. *J Am Coll Cardiol*. 2021;78(16):1621–1631. doi:10.1016/j.jacc.2021.08.018

47. Hoogeveen RM, Pereira JPB, Nurmohamed NS, et al. Improved cardiovascular risk prediction using targeted plasma proteomics in primary prevention. *Eur Heart J*. 2020;41(41):3998–4007. doi:10.1093/eurheartj/ehaa648

48. Nurmohamed NS, Belo Pereira JP, Hoogeveen RM, et al. Targeted proteomics improves cardiovascular risk prediction in secondary prevention. *Eur Heart J*. 2022;43(16):1569–1577. doi:10.1093/eurheartj/ehac055

49. Greener JG, Kandathil SM, Moffat L, Jones DT. A guide to machine learning for biologists. *Nat Rev Mol Cell Biol*. 2022;23(1):40–55. doi:10.1038/s41580-021-00407-0

50. Rhodes JS, Cutler A, Moon KR. Geometry- and Accuracy-Preserving Random Forest Proximities. *IEEE Trans Pattern Anal Mach Intell*. 2023;45(9):10947–10959. doi:10.1109/tpami.2023.3263774

51. Chakraborty A, Li Y, Zhang C, Li Y, LeMaire SA, Shen YH. Programmed cell death in aortic aneurysm and dissection: a potential therapeutic target. *J Mol Cell Cardiol*. 2022;163:67–80. doi:10.1016/j.yjmcc.2021.09.010

52. Zeng T, Shi L, Ji Q, et al. Cytokines in aortic dissection. *Clin Chim Acta*. 2018;486:177–182. doi:10.1016/j.cca.2018.08.005

53. Murakami M, Kamimura D, Hirano T. Pleiotropy and Specificity: insights from the Interleukin 6 Family of Cytokines. *Immunity*. 2019;50 (4):812–831. doi:10.1016/j.immuni.2019.03.027

54. Kang S, Narazaki M, Metwally H, Kishimoto T. Historical overview of the interleukin-6 family cytokine. *J Exp Med*. 2020;217(5).:1 doi:10.1084/jem.20190347

55. Forcina L, Franceschi C, Musarò A. The hormetic and hermetic role of IL-6. *Ageing Res Rev*. 2022;80:101697. doi:10.1016/j.arr.2022.101697

56. Wen D, Zhou XL, Li JJ, et al. Plasma concentrations of interleukin-6, C-reactive protein, tumor necrosis factor-α and matrix metalloproteinase-9 in aortic dissection. *Clin Chim Acta*. 2012;413(1–2):198–202. doi:10.1016/j.cca.2011.09.029

57. Jones SA, Jenkins BJ. Recent insights into targeting the IL-6 cytokine family in inflammatory diseases and cancer. *Nat Rev Immunol*. 2018;18 (12):773–789. doi:10.1038/s41577-018-0066-7

58. Anzai A, Shimoda M, Endo J, et al. Adventitial CXCL1/G-CSF expression in response to acute aortic dissection triggers local neutrophil recruitment and activation leading to aortic rupture. *Circ Res*. 2015;116(4):612–623. doi:10.1161/circresaha.116.304918

59. Ju X, Ijaz T, Sun H, et al. Interleukin-6-signal transducer and activator of transcription-3 signaling mediates aortic dissections induced by angiotensin II via the T-helper lymphocyte 17-interleukin 17 axis in C57BL/6 mice. *Arterioscler Thromb Vasc Biol*. 2013;33(7):1612–1621. doi:10.1161/atvbaha.112.301049

60. Wang D, Day EA, Townsend LK, Djordjevic D, Jørgensen SB, Steinberg GR. GDF15: emerging biology and therapeutic applications for obesity and cardiometabolic disease. *Nat Rev Endocrinol*. 2021;17(10):592–607. doi:10.1038/s41574-021-00529-7

61. Memon AA, Zarrouk M, Ågren-Witteschus S, Sundquist J, Gottsäter A, Sundquist K. Identification of novel diagnostic and prognostic biomarkers for abdominal aortic aneurysm. *Eur J Prev Cardiol*. 2020;27(2):132–142. doi:10.1177/2047487319873062

62. Shelbaya K, Arthur V, Yang Y, et al. Large-Scale Proteomics Identifies Novel Biomarkers and Circulating Risk Factors for Aortic Stenosis. *J Am Coll Cardiol*. 2024;83(5):577–591. doi:10.1016/j.jacc.2023.11.021

63. Zhang Y, Liu Q, Yang S, Liao Q. CD58 Immunobiology at a Glance. *Front Immunol*. 2021;12:705260. doi:10.3389/fimmu.2021.705260

64. Maggi E, Moretta L. Siglec-7, a target for novel therapeutical approaches of Systemic Mastocytosis. *Pharmacol Res*. 2020;158:104731. doi:10.1016/j.phrs.2020.104731

65. Ibarlucea-Benitez I, Weitzenfeld P, Smith P, Ravetch JV. Siglecs-7/9 function as inhibitory immune checkpoints in vivo and can be targeted to enhance therapeutic antitumor immunity. *Proc Natl Acad Sci U S A*. 2021;118(26). doi:10.1073/pnas.2107424118

66. Haas Q, Markov N, Muerner L, et al. Siglec-7 represents a glyco-immune checkpoint for non-exhausted effector memory CD8+ T cells with high functional and metabolic capacities. *Front Immunol*. 2022;13:996746. doi:10.3389/fimmu.2022.996746

67. Radhakrishnan SV, Luetkens T, Scherer SD, et al. CD229 CAR T cells eliminate multiple myeloma and tumor propagating cells without fratricide. *Nat Commun*. 2020;11(1):798. doi:10.1038/s41467-020-14619-z

68. Olson M, Radhakrishnan SV, Luetkens T, Atanackovic D. The role of surface molecule CD229 in Multiple Myeloma. *Clin Immunol*. 2019;204:69–73. doi:10.1016/j.clim.2018.10.006